Exp Brain Res (2009) 193:455–466
DOI 10.1007/s00221-008-1644-x

RESEARCH ARTICLE

Otolith inputs to pursuit neurons in the frontal eye fields of alert monkeys

Teppei Akao · Sergei Kurkin · Junko Fukushima · Kikuro Fukushima

Received: 27 August 2008 / Accepted: 1 November 2008 / Published online: 22 November 2008

Abstract The smooth-pursuit system must interact with the vestibular system to maintain the accuracy of eye movements in space during head movement. Maintenance of a target image on the foveae is required not only during head rotation which activates primarily semi-circular canals but also during head translation which activates otolith organs. The caudal part of the frontal eye fields (FEF) contains pursuit neurons. The majority of them receive vestibular inputs induced by whole body rotation. However, it has not been tested whether FEF pursuit neurons receive otolith inputs. In the present study, we first classified FEF pursuit neurons as belonging to one of three groups (vergence + fronto-parallel pursuit, vergence only, fronto-parallel pursuit only) based on their responses during fronto-parallel pursuit and mid-sagittal vergence-pursuit. We, then, tested discharge modulation of these neurons during fore/aft and/or right/left translation by passively moving the whole body sinusoidally at 0.33 Hz (±10 cm, peak velocity 19 cm/s; 0.04g). The majority of FEF pursuit neurons in all three groups were activated by fore/aft and right/left translation without a target in complete darkness. There was no correlation between the magnitude of discharge modulation and translational vestibulo-ocular reflex (VOR). Preferred directions of translational responses were distributed nearly evenly in front of the monkeys. Discharge modulation was also observed when a target moved together with whole body, requiring the monkeys to cancel the translational VOR. These results indicate that the discharge modulation of FEF pursuit neurons during whole body translation reflected otolith inputs.

Keywords Frontal eye fields · Pursuit neurons · Smooth-pursuit · Vergence-pursuit · Otolith inputs · Translation · Monkey

T. Akao · S. Kurkin · K. Fukushima (✉)
Department of Physiology,
Hokkaido University School of Medicine,
West 7, North 15, Sapporo 060-8638, Japan
e-mail: kikuro@med.hokudai.ac.jp

J. Fukushima
Department of Health Sciences,
Hokkaido University School of Medicine,
Sapporo 060-8638, Japan

Introduction

The smooth-pursuit system has evolved in primates to maintain the image of a slowly moving object of interest on the foveae of both eyes during movement. During head movements, the pursuit system must interact with the vestibular system to maintain the accuracy of eye movements in space so that eye-velocity-in-space (i.e., gaze velocity) matches target velocity (see Leigh and Zee 2006 for a review). The VOR is well known to have an important role in stabilizing a visual image on the retina by compensating for head movements. Maintenance of a target image on the foveae is required not only during head rotation which activates primarily semi-circular canals but also during head translation which activates otolith organs. The translational VOR requires compensation different from the rotational VOR (Tomko and Paige 1992; Angelaki et al. 2001). This is because the geometrical relationship between the target and the eyes with respect to the direction of translation critically determines the amount of compensation needed to stabilize the target image on the foveae (see Angelaki 2004 for a review).

The caudal part of the frontal eye fields (FEF) contains pursuit-related neurons (pursuit neurons, MacAvoy et al. 1991; Gottlieb et al. 1993, 1994; Tian and Lynch 1996a, b; Tanaka and Fukushima 1998; Fukushima et al. 2000, 2002a, b; Tanaka and Lisberger 2002). The majority of FEF pursuit neurons receive vestibular inputs induced by passive whole body rotation that activates primarily semicircular canals (Fukushima et al. 2000; Akao et al. 2007). However, otolith inputs to FEF pursuit neurons have not been tested. Projection of otolith (i.e., saccular) signals to the FEF have been reported only recently by using functional magnetic resonance imaging in humans (Miyamoto et al. 2007).

As a first step to examine the role of otolith signals in the caudal FEF, in this study we asked whether FEF pursuit neurons receive otolith inputs. For this, we tested responses of FEF pursuit neurons during passive horizontal translation of the whole body in complete darkness. Discharge modulation was compared when a target was presented during translation. Some of the results have been presented in preliminary form (reviews K. Fukushima et al. 2005; J. Fukushima et al. 2006).

Materials and methods

Two Japanese monkeys (*Macaca fuscata*, H, K, 3.9 and 4.5 kg) provided data for this study. All procedures were performed in strict compliance with the guidelines for the Care and Use of Animals of National Institutes of Health. Our specific protocols were approved by the Animal Care and Use Committee of Hokkaido University School of Medicine. The general methods for animal preparation, training, vestibular stimulation, recording, and data analysis were described in detail previously (Fukushima et al. 2000, Akao et al. 2005). Briefly, each monkey was sedated with ketamine hydrochloride (5 mg/kg, i.m.), and then anesthetized with sodium pentobarbital (25 mg/kg, i.p.). Additional anesthesia (0.5–1.0% halothane mixed with 50% nitrous oxide and 50% oxygen) was administered as necessary. Under aseptic conditions, head holders were installed to restrain the head firmly in the primate chair. A scleral search coil was implanted on each eye to record vertical and horizontal components of eye movement for both eyes (Fuchs and Robinson 1966). Analgesics and antibiotics were administered post-surgically.

Each monkey was seated in a primate chair in darkness with the head restrained in the stereotaxic plane, facing a 22 in. computer display (Mitsubishi, RDF 221S) placed 65 cm away from the eyes (Fig. 1a, 0° orientation). The inter-ocular distances of the 2 monkeys were 20 and 21 mm. A red spot of 0.2° angular size was presented at the screen distance. Eye position signals were calibrated for each eye separately by requiring the animal to fixate a stationary spot or pursue a slowly moving one at 0.2 Hz (±10°). Visual stereo stimuli were generated as two alternating images viewed by left or right eyes through polarization shutter glasses that were switched at 120 Hz rate as described previously (Akao et al. 2005). The monkeys were trained with apple juice reward for pursuing the spot that moved in fronto-parallel plane or in depth. After this training, a recording chamber was installed over craniotomy (anterior 21–25; lateral 10–15 mm) to allow single neuron recording in the left peri-arcuate cortical area.

Recording procedures

The primate chair was attached to a turntable for rotation. The turntable together with the chair was mounted on a linear sled that moved sinusoidally (Fig. 1a). Pursuit neurons were recorded extracellulary mostly in the fundus of the arcuate sulcus (see " Results"). For our search stimulus, the target moved sinusoidally along oblique trajectories that were generated by combinations of target motion in fronto-parallel plane and in depth (3D-pursuit) at 0.5 Hz (±10°), and monkeys were required to pursue the spot (Fig. 1a, 0° orientation). Once responsive single neurons were encountered as judged visually and on the audio monitor, neuronal responses were tested during fronto-parallel pursuit in 4 planes (vertical, horizontal, and two diagonals, separated by 45°) at the screen distance and during vergence-pursuit in the mid-sagittal plane from 65 to 10 cm depth. This was to examine whether responsive neurons discharged during fronto-parallel pursuit only, vergence-pursuit only, or both. (e.g., Fukushima et al. 2002a; Akao et al. 2005).

Whole body translation was applied by moving the chair sinusoidally at 0.33 Hz (±10 cm, peak velocity and acceleration, 19 cm/s and 40.0 cm/s/s = 0.04g, respectively) along a given axis without a target in complete darkness to minimize pursuit related discharge modulation while the monitor was turned off (Fig. 1a). All pursuit neurons identified ($n = 68$) were tested for fore/aft translation (Fig. 1a, 0° orientation, Table 1Ba). Thirty neurons of the 68 were also tested for right/left translation (Table 1Bb) by positioning the chair (and hence the monkey) at ±90° orientation as schematically illustrated in Fig. 1a. Preferred directions for translational responses were examined in 23 neurons by positioning the monkey at ±45° orientation (Fig. 1a) so that translation was tested along 4 axis (right/left, fore/aft, ±45°). For 10 of the 23 neurons the monkeys were oriented at ±30° also. The monkeys were then oscillated along the same earth-horizontal direction so that whole body translation was applied along different directions with respect to the animals' body. This was to reconstruct responses to translation relative to the animals' body as schematically illustrated in Fig. 1b. The monkeys were not required to

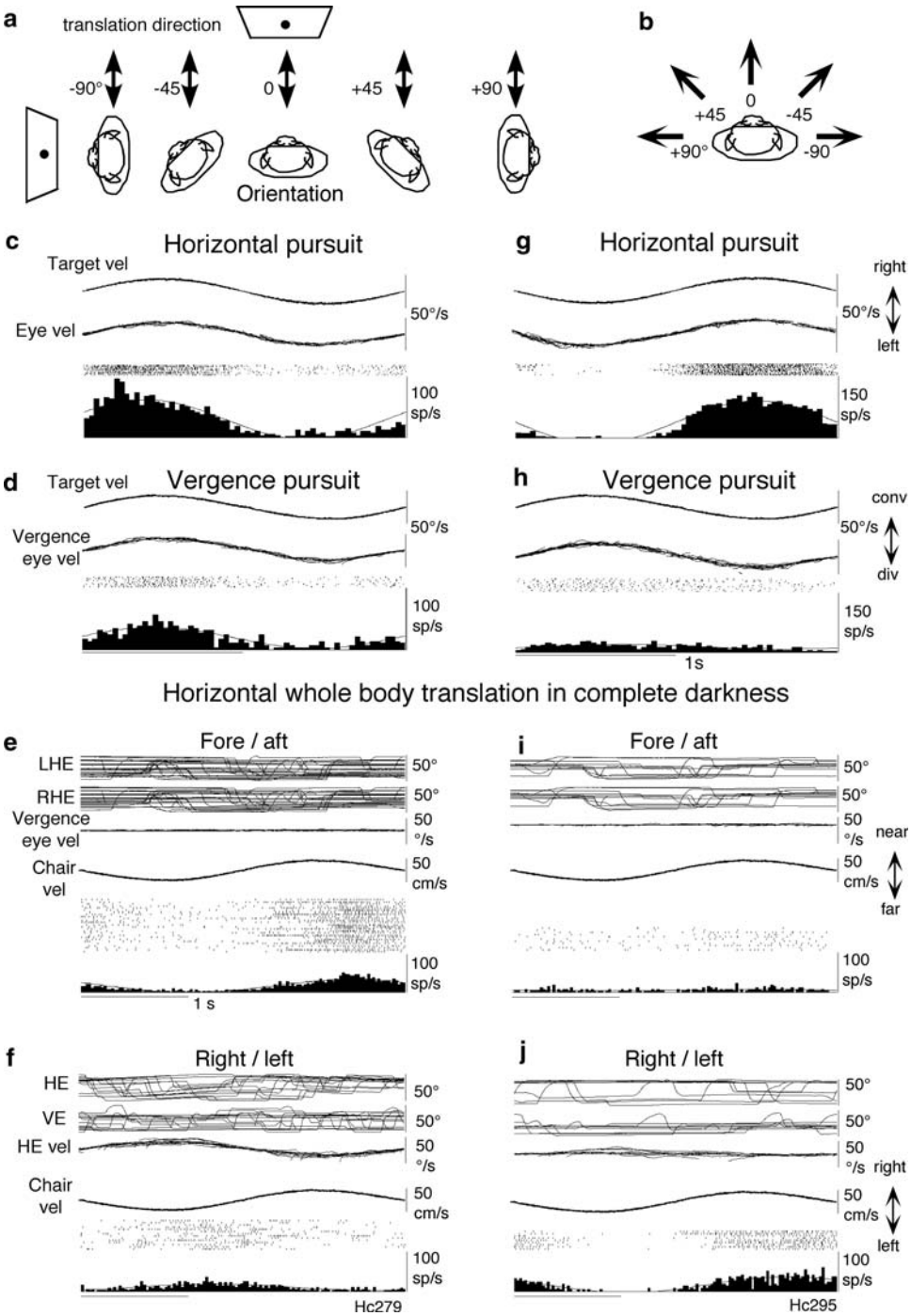

Fig. 1 Methods to test whole body translation and discharge of representative FEF pursuit neurons. **a** Schematic illustration of the direction of passive whole body translation and orientation of monkeys while identical sinusoidal translation was applied without a target in complete darkness in the same direction pointed by *arrows*. **b** Direction of horizontal translation with respect to the monkeys. **c–f**, **g–j** are two different neurons. **c**, **g** Discharge during horizontal pursuit, **d** and **h** discharge during vergence-pursuit. **e**, **i** Discharge during fore/aft translation. **f**, **j** Discharge during right/left translation. From *top* to *bottom* in **c**, **d** and **g**, **h** are superimposed target velocity (vel), "de-saccaded" horizontal eye velocity (eye vel) and "de-saccaded" vergence eye velocity with the overlaid fit sine waves, spike rasters, and histograms of cell discharge with superimposed fit sine waves. From *top* to *bottom* in **e**, **i** are left horizontal and right horizontal eye positions (LHE, RHE, respectively), "de-saccaded" vergence eye velocity, chair velocity and cell discharge with superimposed fit sine waves. From *top* to *bottom* in **f**, **j** are horizontal and vertical eye position (HE, VE, respectively), horizontal eye velocity (HE vel), chair velocity and cell discharge with superimposed fit sine waves. All traces in **c–j** were superimposed with respect to the stimulus (target or chair) velocity. For further explanation, see text

perform any particular task during this condition but were kept alert by occasional randomly delivered drops of apple juice.

In 14 FEF pursuit neurons, we presented a target on another computer monitor during right/left translation (Fig. 1a, −90° orientation). This monitor was placed 50 cm in front of the monkeys. Two task conditions were tested. In one, the target moved together with the whole body, requiring cancellation of the translational VOR. In the other, the target remained stationary in space, requiring perfect compensation by translational VOR (VOR ×1). Peak horizontal eye velocity for perfect compensation that was required by the geometrical relationship between the target and the eyes during right/left translation at 0.33 Hz (±10 cm) was 23.4 deg/s.

Responses of these neurons were also tested during fore/aft translation for VOR cancellation and VOR ×1 at 0° orientation with the target distance of 65 cm (Fig. 1a). Peak vergence eye velocity for perfect compensation required by the geometrical relationship between the target and the eyes

Table 1 Number of FEF pursuit neurons tested for 3D-pursuit and passive whole body translation

A. 3D-Pursuit	*n*
Fronto-parallel pursuit + vergence-pursuit	44
Vergence-pursuit only	18
Fronto-parallel pursuit only	6
Total	68
B. Number of pursuit neurons responsive to horizontal whole body translation in complete darkness	
a. Fore/aft translation	44/68 = 65%
Fronto-parallel pursuit + vergence-pursuit	34/44
Vergence-pursuit only	6/18
Fronto-parallel pursuit only	4/6
b. Right/left translation	24/30 = 80%
Fronto-parallel pursuit + vergence-pursuit	19/21
Vergence-pursuit only	2/5
Fronto-parallel pursuit only	3/4

A, number of three groups of neurons tested. B, number of pursuit neurons responsive to fore/aft (Ba) and right/left (Bb) translation among tested neurons and percentages of responsive neurons

during fore/aft translation at 0.33 Hz (±10 cm) was 0.6 deg/s. Horizontal-pursuit and/or vergence-pursuit were also tested at 0.3 Hz (±10°, peak velocity 18.8 deg/s) and 0.5 Hz (±5°, peak velocity 15.7 deg/s) for comparison.

In 10 of the 14 neurons, we compared rotational VOR cancellation and VOR ×1 by applying whole body rotation in the horizontal (yaw) plane at 0.3 Hz (±10°). During rotational VOR cancellation, the target moved together with the whole body. During rotational VOR ×1, the target remained stationary in space, requiring perfect compensation by VOR (VOR ×1) as previously described (Miles and Fuller 1975; Lisberger and Fuchs 1978; Fukushima et al. 2000; Akao et al. 2007). These neurons were also tested during whole body rotation without a target in complete darkness.

Data analysis

The data were analyzed off-line as previously described (Fukushima et al. 2000, 2002a, b; Akao et al. 2005). Discharge of individual neurons was discriminated with a dual time–amplitude window discriminator and digitized together with eye position, chair position and target position signals at 500 Hz using a 16-bit A/D board. Eye position signals were differentiated by analog circuits (DC—100 Hz, −12 dB/octave) to obtain eye velocity. Stimulus position signals were differentiated by software to obtain velocity. During vergence-pursuit and during fore/aft translation in complete darkness, vergence eye movements were calculated as the difference between the horizontal components of the left and right eyes (e.g., Akao et al. 2005). To examine vergence-pursuit and fronto-parallel pursuit eye velocity, saccades on eye velocity traces and blink-related fast eye movements were removed using our interactive computer program (Fukushima et al. 2000). Some FEF pursuit neurons analyzed in this study exhibited burst of spikes during blinks and saccades with the presence of a tracking target. We deleted those traces entirely from the analysis.

All traces were aligned with stimulus velocity for 10–30 cycles, and raster and histograms of neuronal responses were constructed. To quantify responses, each cycle was divided into 128 equal bins. A sine function was fit to averaged velocities and cycle histograms of neuronal discharge, exclusive of the bins with zero spikes, by means of a least-squared error algorithm. Responses that had a harmonic distortion (HD) of less than 50% or a signal to noise ratio (S/N) of higher than 1.0 were selected for further analysis; S/N was defined as the amplitude of the fundamental frequency component divided by the amplitudes of the 3rd through 8th harmonic, and HD as the amplitude of the 2nd harmonic divided by that of the fundamental (Wilson et al. 1984). The phase-shift of the peak of the fit-function relative to peak upward/rightward or forward stimulus velocity was calculated as a difference in degrees. For neuronal responses during vergence-pursuit, phase shift of neuronal responses was calculated relative to peak convergence target/eye velocity. For fore/aft and right/left translation, phase shift was calculated relative to peak forward and rightward chair velocity, respectively. Sensitivity (re stimulus velocity) was calculated as the peak amplitude of the fundamental component fit to the cycle histogram divided by the peak amplitude of the fit stimulus velocity (i.e., target velocity for fronto-parallel pursuit and vergence-pursuit, chair velocity during translation). Sensitivity (re stimulus velocity) ≥0.10 spikes/s/deg/s was taken as significant modulation (Fukushima et al. 2000, 2002a, b). Vergence eye velocity and horizontal eye velocity responses were calculated similarly (Akao et al. 2005).

Preferred directions were examined by comparing sensitivity (relative to chair velocity) during translation in different orientations in complete darkness without a target (Fig. 1a, b). A Gaussian function was used to estimate preferred directions (Colby et al. 1993; Gottlieb et al. 1994) by plotting mean discharge rate against different directions with respect to the monkey (Fig. 1b).

Histological procedures

Near the conclusion of recordings, the sites of pursuit neuron recordings were marked and were confirmed as reported previously (Tanaka and Fukushima 1998; Fukushima et al. 2000, 2002a, b).

Results

This study examined effects of horizontal whole body translation on a total of 68 FEF pursuit neurons. We first classified these neurons as belonging to one of three groups based on their responses of whether they discharged during fronto-parallel pursuit, vergence-pursuit, or both (see "Materials and methods"). As summarized in Table 1A, the majority of them (44/68 = 65%) responded to both frontal-parallel pursuit and vergence-pursuit. The two columns in Fig. 1c–f, g–j illustrate discharge of 2 representative FEF pursuit neurons during different stimulus conditions. The neuron shown on the left responded during both fronto-parallel pursuit (Fig. 1c) and vergence-pursuit (Fig. 1d). Neurons that responded during vergence-pursuit but not during fronto-parallel pursuit (18/68 = 26 %) or those that responded during fronto-parallel pursuit but not during vergence-pursuit (6/68 = 9 %, Fig. 1g vs. h) were also examined, although such neurons were in the minority in this study (Table 1A). We, first, anayzed discharge modulation of these neurons during fore/aft and/or right/left translation without a target in complete darkness (see "Materials and methods").

Responses of FEF pursuit neurons to passive horizontal translation of the whole body in complete darkness

As summarized in Table 1B, the majority of tested neurons responded to both fore/aft (44/68 = 65%, Table 1Ba) and right/left translation (24/30 = 80%, Table 1Bb). The responsive neurons include all 3 types of FEF pursuit neurons (fronto-parallel pursuit + vergence-pursuit, vergence-pursuit only, and fronto-parallel pursuit only neurons, Table 1B). The example neuron shown in the left column of Fig. 1c–f discharged during forward translation (Fig. 1e) and leftward translation (Fig. 1f). In contrast, the neuron shown in the right column of Fig. 1g–j was activated during rightward translation (Fig. 1j) but not during fore/aft translation (Fig. 1i).

To examine whether fore/aft translation in complete darkness without a target induced vergence eye movement responses, we measured vergence eye velocity (see "Materials and methods"). Vergence eye velocity was induced minimally (less than 1 deg/s, typically 0.7 deg/s) during fore/aft translation (Fig. 1e, i). In contrast, right/left translation induced horizontal eye movement responses more consistently (Fig. 1f, j). However, the magnitudes of horizontal eye velocity varied widely from 1.4 to 19.7 deg/s with the mean of 12.3 (±5.4) deg/s without a target. The expected peak horizontal eye velocity for perfect compensation if a stationary target in space had been presented during right/left translation was 23.4 deg/s at a target distance of 50 cm (see " Materials and methods"), suggesting that without a target our monkeys exhibited the mean horizontal translational VOR gain of 0.53 (=12.3/23.4).

To examine discharge characteristics of FEF pursuit neurons during horizontal translation, Fig. 2a, b plots sensitivity of responsive neurons against phase shift (re chair velocity) during fore/aft translation (Fig. 2a) and right/left translation (Fig. 2b). Mean sensitivity tended to be higher for responses during right/left translation than fore/aft (mean 1.03 vs. 0.51 sp/s/cm/s, respectively). Phase values were distributed widely, but the majority were scattered around peak chair velocity (−45 to +45°, −135 to −180°, or 135 to 180°, Fig. 2a, b).

Because the majority of tested neurons responded during vergence-pursuit (Table 1A) and also during fore/aft translation (Table 1Ba), we examined whether there was any functional correlation between the directions and/or magnitudes of the two kinds of responses. The activation of the example neuron illustrated in Fig. 1c–f during forward and leftward translation (Fig. 1e, f) is consistent with the activation of this neuron during convergence (Fig. 1d) and rightward pursuit (Fig. 1c). However, rightward pursuit preferred directions of the neuron illustrated in Fig. 1g–j is not consistent with the activation of this neuron during rightward translation (Fig. 1j), because during rightward translation the compensatory VOR rotated the eyes toward left (see also below).

Figure 2c plots sensitivity to chair velocity during fore/aft translation against vergence eye velocity sensitivity of each neuron (n = 68). For fore/aft responses, positive and negative values indicate responses during forward and backward translation, respectively. For vergence response, convergence and divergence responses were plotted as positive and negative values, respectively. There was no correlation between sensitivity to translation and vergence-pursuit (Fig. 2c). A similar result was obtained by plotting values only for neurons that responded during vergence-pursuit and that also responded during fore/aft translation (n = 36, Fig. 2d). In Fig. 2e, we re-plotted the absolute values of sensitivity to fore/aft translation and vergence-pursuit. There was no correlation between the two. Similarly, we examined whether there was any correlation between sensitivity to chair velocity during right/left translation and eye velocity sensitivity during horizontal pursuit of FEF neurons with horizontal preferred directions. As plotted in Fig. 2f for 20 horizontal pursuit neurons, there was no significant correlation between the two. We also tested whether neuronal response to right/left translation was a result of translational VOR that was observed more consistently than that during fore/aft translation as described above. As plotted in Fig. 2g, there was no significant correlation between response sensitivity to chair velocity during right/left translation and translational VOR for all neurons

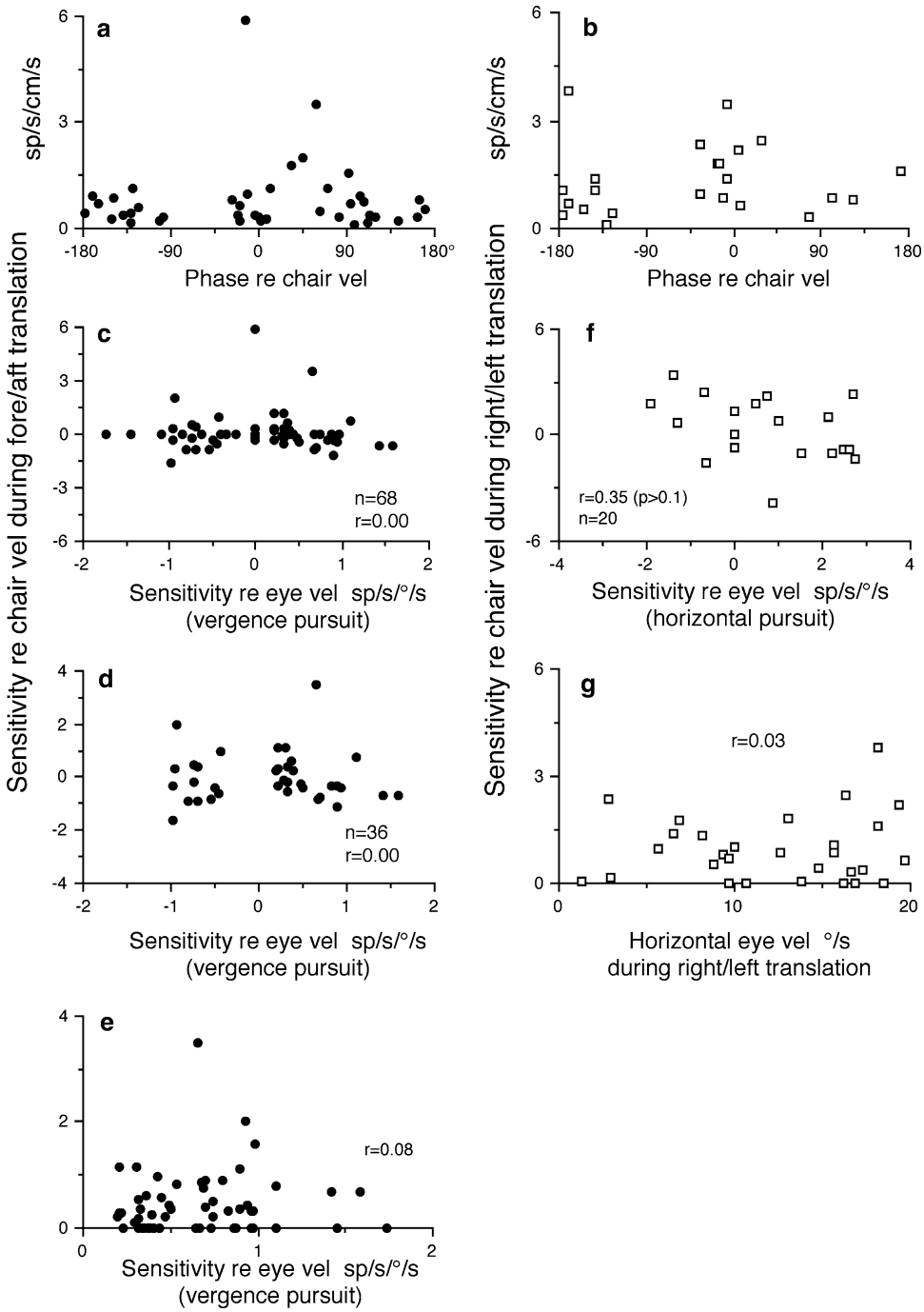

Fig. 2 Discharge characteristics of FEF pursuit neurons during horizontal whole body translation. **a**, **b** Sensitivity plotted against phase shift (re chair velocity) of individual responsive neurons during fore/aft translation (**a**) and right/left translation (**b**). **c** Sensitivity (re chair velocity) during fore/aft translation plotted against sensitivity (re eye velocity) during vergence-pursuit for all neurons tested (n = 68). Positive and negative values on the ordinate indicate that discharge increased during forward and backward translation, respectively. Positive and negative values on the abscissa indicate convergence and divergence responses, respectively. **d** Similar plot to **c** but only for neurons that responded during vergence-pursuit and that also responded during fore/aft translation. **e** Plots absolute values of sensitivity to fore/aft translation against vergence eye velocity sensitivity. **f** Sensitivity (re chair velocity) during right/left translation plotted against sensitivity (re eye velocity) during horizontal pursuit for 20 horizontal pursuit neurons. Positive and negative values on the ordinate indicate that discharge increased during rightward and leftward translation, respectively. Positive and negative values on the abscissa indicate response during rightward and leftward pursuit, respectively. **g** Sensitivity (re chair velocity) of neuronal responses during right/left translation plotted against simultaneously recorded horizontal eye velocity

tested. These results suggest that responses induced by fore/aft and right/left translation and vergence/fronto-parallel pursuit responses (Fig. 2c–e, f, g) were mostly independent in FEF pursuit neurons (see "Discussion").

Preferred directions of FEF pursuit neurons during passive horizontal translation in complete darkness

Because the majority of FEF pursuit neurons tested responded to both fore/aft translation and right/left translation (Table 1B), we examined preferred directions of translational responses in 23 neurons by applying whole body translation in 8 or more directions in complete darkness (Fig. 1a, b, see "Materials and methods"). Figure 3 illustrates responses of two representative neurons to translation while the orientation of the monkeys was systematically changed (Fig. 1a). The neuron shown in Fig. 3a, b was the same neuron shown in Fig. 1c–f and exhibited stronger modulation when translation was applied while the animal was oriented at +45° (Figs. 1b, 3b). The modulation was minimal when the animal was oriented at −45° (Fig. 3b)

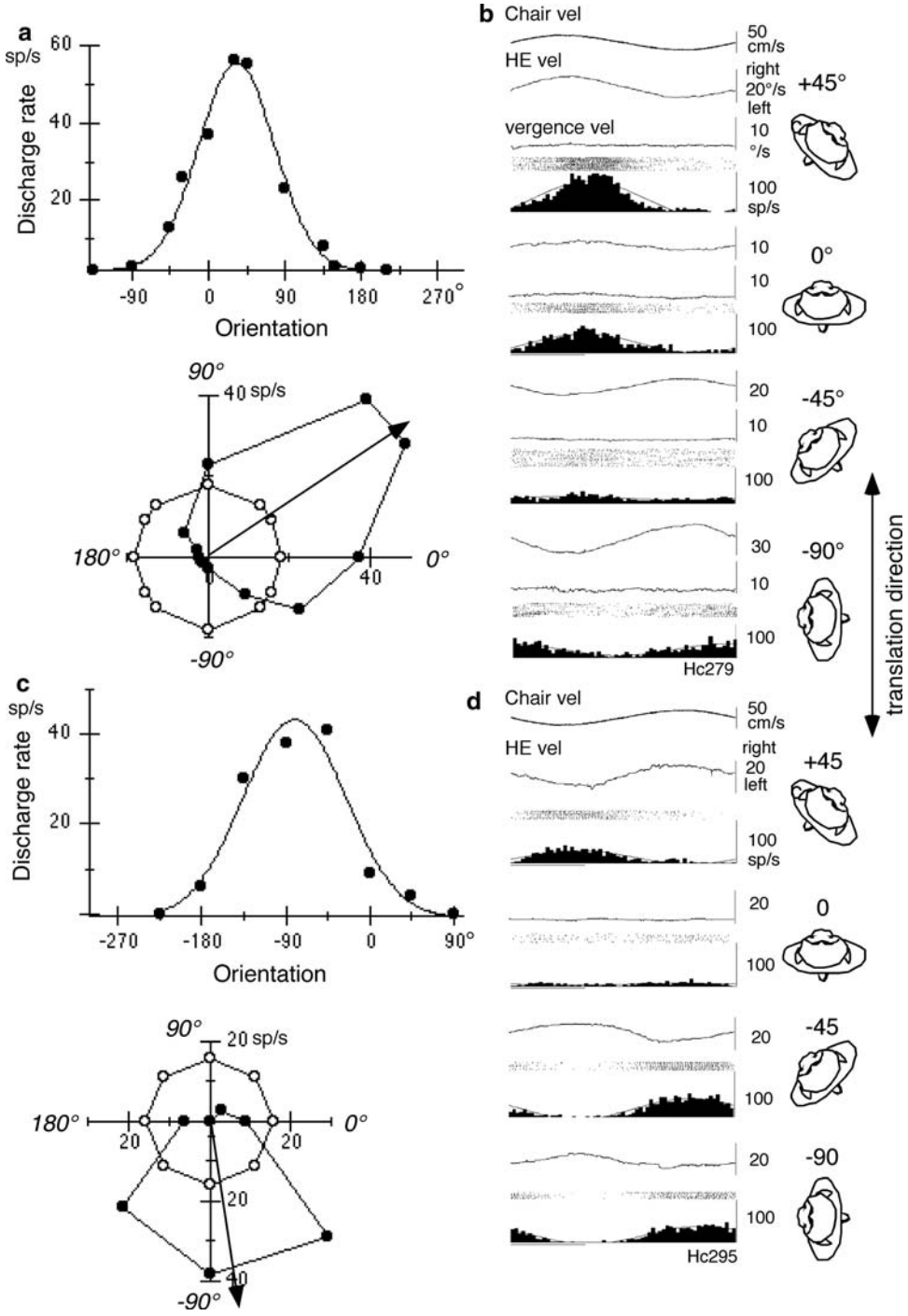

Fig. 3 Directional tuning and Gaussian fit of representative FEF pursuit neurons during whole body translation in complete darkness. **a**,**b** and **c**, **d** are two different neurons. *Filled circles* in **a** and **c** plot discharge rate against translation direction with respect to the monkey. *Open circles* are resting discharge rate while the chair was stationary in space. Preferred directions calculated by Gaussian fit are indicated by *arrows* in **a**, **c**. **b**, **d** Spike rasters and histograms of cell discharge with superimposed fit sine waves while the horizontal orientation of the animal was selected by positioning the chair at different orientations. Simultaneously recorded mean horizontal eye velocity (HE vel) and vergence eye velocity (vergence vel) are shown in **b** at different orientations. Notice different gain scales for horizontal eye velocity. Only mean HE vel is shown for **d** at different orientations. Chair velocity is identical for each neuron at different orientations and is shown only at +45° orientation in **b**, **d**. For details, see Fig. 1a, b

and the response phase (re chair velocity) reversed when the animal was oriented at −90°. The preferred direction calculated by the Gaussian fit was 33° (Fig. 3a). In contrast, the neuron shown in Fig. 3c, d exhibited stronger modulation when the animal was oriented at −45 and −90°, and the modulation was minimal at 0° and response phase reversed at +45°. The estimated preferred orientation by the Gaussian fit was −81° (Fig. 3c). This neuron was the same neuron shown in Fig. 1g–j.

Figure 3b, d also illustrates simultaneously recorded mean horizontal eye velocity (HE vel) and vergence eye velocity (vergence vel, Fig. 3b). Discharge of these neurons during translation at different orientation cannot be explained by translational VOR alone. Both neurons discharged strongly during rightward pursuit (Fig. 1c, g), but the neuron shown in Fig. 3b discharged very differently during translation at +45° and −45° orientation, despite the fact that the magnitude of the translational horizontal eye

velocity was virtually identical with minimal vergence eye velocity (Fig. 3b). At −90°orientation, translational horizontal eye velocity was largest but this neuron discharged weakly during this orientation (Fig. 3b) compared to the discharge at +45° orientation. The neuron shown in Fig. 3d also exhibited a clear dissociation during smooth-pursuit and translational VOR. Despite the fact that preferred direction of this neuron during fronto-parallel pursuit was rightward (Fig. 1g), it discharged strongly during leftward VOR during translation at +45°, −45° and −90° orientations (Fig. 3d). These results suggest that otolith inputs contributed to the discharge of FEF pursuit neurons during translation (see below and "Discussion").

Figure 4 plots preferred directions of the 23 neurons for translational responses. Preferred directions were distributed nearly evenly in front of the monkeys. In our small sample, we rarely obtained neurons with preferred directions oriented backward of the monkeys (Fig. 4, $n = 23$).

Responses of FEF pursuit neurons during translational VOR cancellation and VOR ×1

To further examine whether neuronal responses during right/left translation was a result of eye velocity sensitivity due to the translational VOR, we tested responses of 14 neurons during right/left translation with a target (Fig. 1a, −90° orientation, see "Materials and methods"). In one condition, the target moved together with the whole body, requiring cancellation of the translational VOR. In the other, the target remained stationary in space, requiring perfect compensation (VOR ×1). In 13 of the 14 neurons tested, discharge modulation was clearly observed during

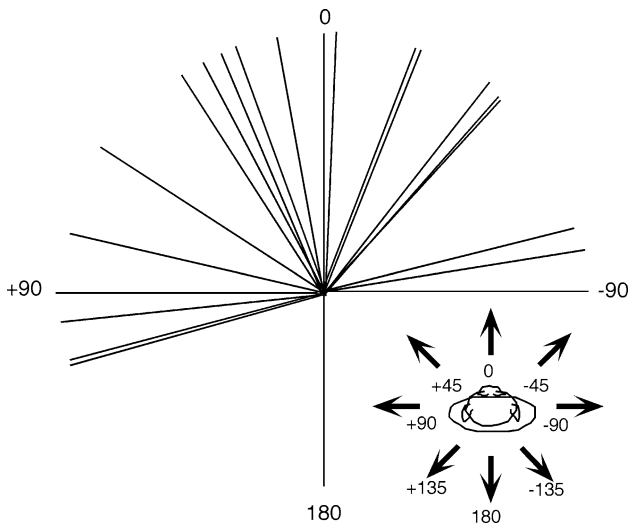

Fig. 4 Preferred directions of translational responses. Preferred directions were calculated for 23 FEF pursuit neurons by Gaussian fit. For further explanation, see text

translational VOR cancellation during which peak horizontal eye velocity was typically less than 2 deg/s (mean 1.8 deg/s). Discharge of two neurons is shown in Fig. 5a, b, f, g. Like these neurons, in 7 of the 13 neurons, amplitudes of discharge modulation during translational VOR cancellation were similar to those during horizontal pursuit (Fig. 5a vs. b, f vs. g) but were larger than those during translational VOR ×1 (Fig. 5b vs. c, g vs. h). Peak horizontal eye velocity during translational VOR ×1 (mean 24.2 deg/s, gain 24.2/23.4 = 1.03) was more than 10 times larger than that during translational VOR cancellation (mean 1.8 deg/s, Fig. 5c vs. b, h vs. g). Mean sensitivities (re chair velocity) of the 7 neurons during translational VOR cancellation and VOR ×1 were 1.57 and 0.82 sp/s/cm/s, respectively. Mean eye velocity sensitivity of these neurons during horizontal pursuit was 1.60 sp/s/deg/s.

Mean discharge rate of the seven neurons are summarized in Fig. 6a, b during right/left translational VOR cancellation (a, red) and VOR ×1 (b, black) and horizontal pursuit (a, black) at 0.3 Hz. Discharge modulation during horizontal pursuit and translational VOR cancellation was similar and were clearly larger than the modulation during translational VOR ×1. For comparison, Fig. 6b (green) plots mean discharge rate during right/left translation without a target in complete darkness. Modulation was clear, although it was smaller than the modulation during translational VOR cancellation (Fig. 6b: green vs. a: red). Discharge modulation of the remaining six neurons during translational VOR cancellation tended to be smaller than that during VOR ×1, but larger than the modulation during translation without a target in complete darkness. Mean sensitivities (re chair velocity) of these neurons during translational VOR cancellation and VOR ×1 were 0.91 and 1.03 sp/s/cm/s, respectively. These results indicate that discharge modulation during right/left translation was not the result of translational VOR.

Figure 5k–m, n, o illustrates discharge of two neurons during fore/aft translation. These neurons discharged during convergence (Fig. 5k) or divergence (Fig. 5n). During fore/aft translational VOR cancellation, mean vergence eye velocity was 0.03 deg/s (Fig. 5l, o), but both neurons were clearly activated when whole body moved backward (Fig. 5l, o) with the discharge modulation comparable to the modulation during vergence-pursuit (Fig. 5k, n). During translational VOR ×1 at a target distance of 65 cm (Fig. 5m), the peak vergence eye velocity was 0.63 deg/s as required by the geometrical relationship between the target and the eyes (see "Materials and methods"). During this condition, amplitude of modulation of this neuron was 15 sp/s (Fig. 5m). The amplitude of modulation of the same neuron during vergence-pursuit (Fig. 5k) was 17 sp/s with the peak vergence eye velocity of 16 deg/s. If the discharge modulation of this neuron during translational VOR ×1

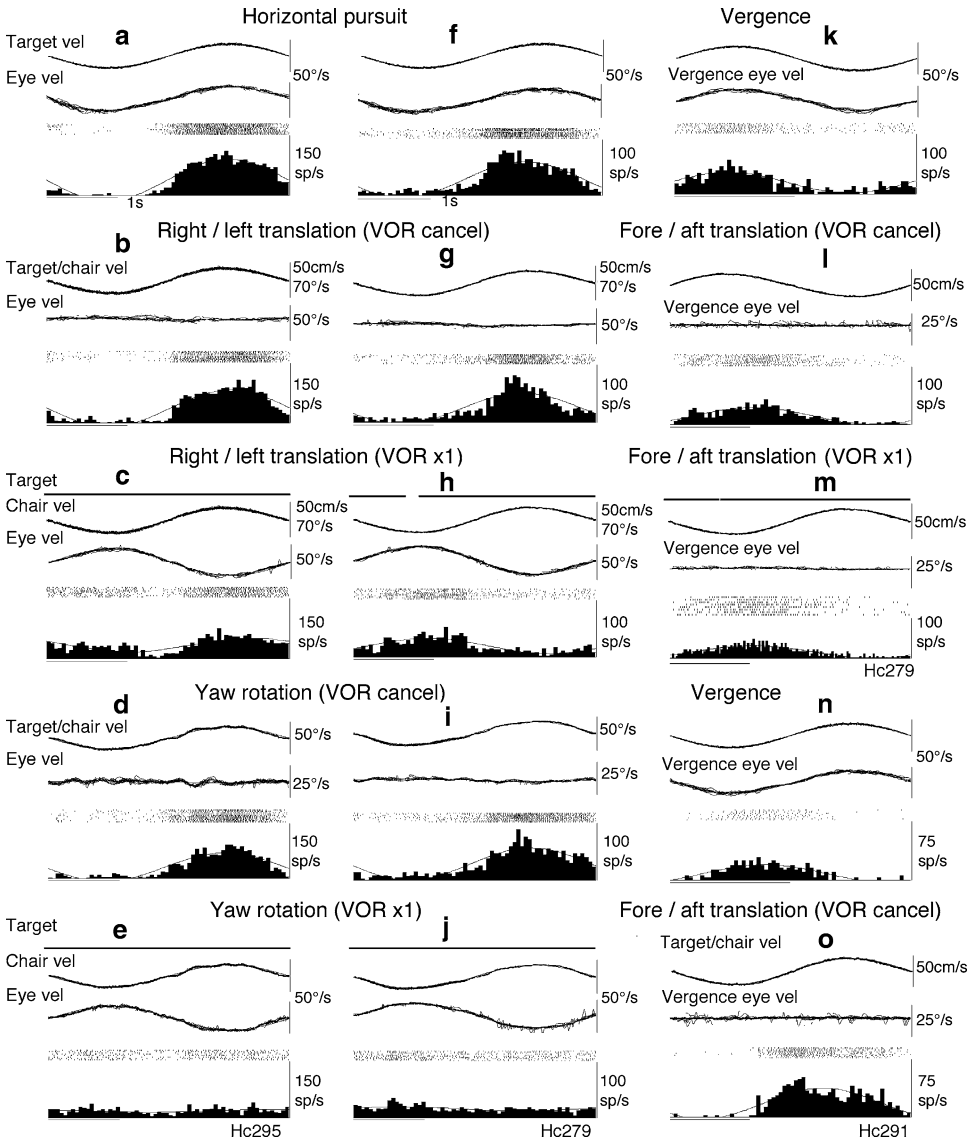

Fig. 5 Responses of FEF pursuit neurons during translational and rotational VOR cancellation and VOR ×1. Discharge of 3 neurons is shown (**a**–**e**, **f**–**m**, **n**–**o**) during horizontal pursuit (**a**, **f**), vergence-pursuit (**k**, **n**), VOR cancellation during right/left translation (**b**, **g**), VOR cancellation during fore/aft translation (**l**, **o**), VOR ×1 during right/left translation (**c**, **h**), VOR ×1 during fore/aft translation (**m**), rotational VOR cancellation (**d**, **i**), and rotational VOR ×1 (**e**, **j**). In each, the *top* trace is target velocity which was identical to chair velocity during VOR cancellation. The *bottom* two traces are spike rasters and averaged histograms of cell discharge with superimposed fit sine waves during smooth-pursuit. Other traces are as labeled. For further explanation, see text

(Fig. 5m) had been a result of vergence eye velocity sensitivity, the expected amplitude of modulation should have been 17/16 × 0.63 = 0.67 sp/s. Our results showing that the actual amplitude of modulation was 15 sp/s (Fig. 5m) indicate that it cannot be accounted for by vergence eye velocity sensitivity alone due to translational VOR. Mean amplitudes of discharge modulation of 14 neurons during fore/aft translational VOR cancellation and VOR ×1 were 7.8 and 6.8 sp/s, respectively (e.g., Fig. 5l, m). These are only slightly smaller than the mean amplitude of modulation of these neurons during vergence-pursuit (9.0 sp/s) despite the clear difference in peak vergence eye velocity (0.03–0.63 vs. 16–17 deg/s, e.g., Fig. 5k–m). These results also suggest contribution of otolith inputs to the discharge modulation during right/left and fore/aft translation (see "Discussion").

Comparison with passive whole body rotation

We compared discharge of 10 of the above 14 neurons during rotational VOR cancellation and VOR ×1 (see "Materials and methods"). Discharge of 2 neurons (Fig. 5a, f) during horizontal rotation is shown in Fig. 5d, e, i, j. Both neurons exhibited discharge during rotational VOR cancellation (Fig. 5d, i), similar to that during horizontal pursuit (Fig. 5a, f) and modulation during rotational VOR ×1 was minimal (Fig. 5e, j). Similar discharge pattern was observed in 6 neurons. These neurons also discharged during translational VOR cancellation (Fig. 6a). Mean discharge rate of the 6 neurons during rotational VOR cancellation, VOR ×1 and chair rotation without a target in complete darkness are shown in Fig. 6c, d. Discharge modulation of these neurons during translational and rotational

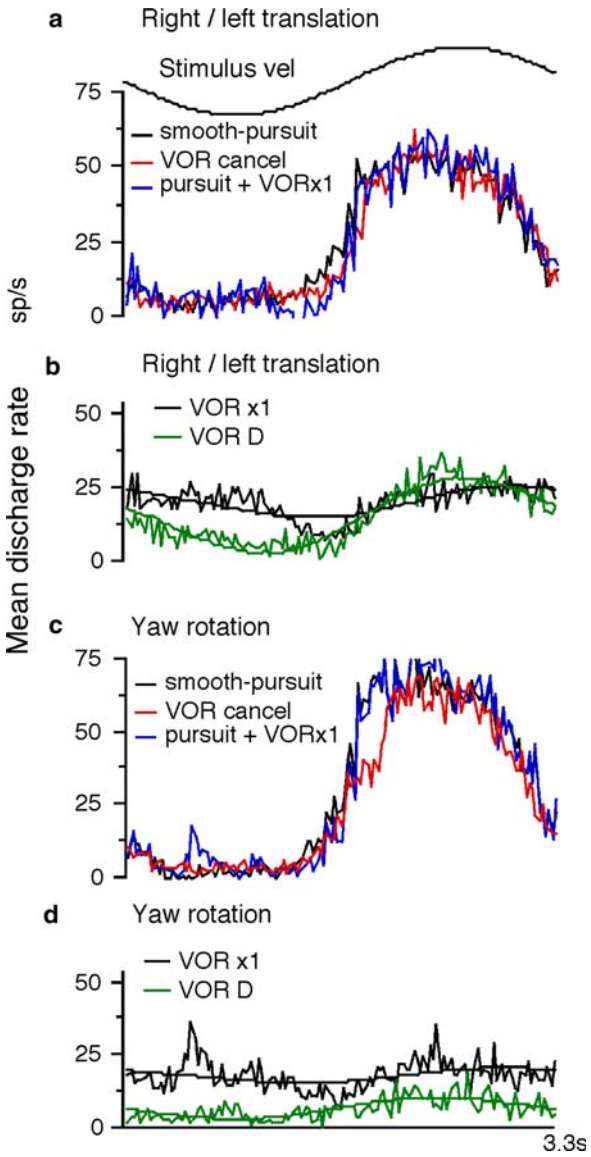

Fig. 6 Mean discharge rate of FEF pursuit neurons during translational and rotational VOR cancellation, VOR ×1 and smooth-pursuit. **a** and **b** show mean response of 7 neurons. **c** and **d** show mean response of 6 neurons, during horizontal pursuit (**a**, **c** *black*), right/left translational VOR cancellation (**a**, *red*) and VOR ×1 (**b**, *black*), right/left translation without a target in complete darkness (**b**, VOR D, *green*), rotational VOR cancellation (**c**, *red*) and VOR ×1 (**d**, *black*), and yaw rotation without a target in complete darkness (**d**, *green*). Predicted modulation during translational VOR cancellation is shown in **a** in *blue* by adding discharge during smooth-pursuit and translational VOR ×1. Predicted modulation during rotational VOR cancellation is shown in **c** in *blue* by adding discharge during smooth-pursuit and rotational VOR ×1. Mean resting discharge rate during fixation of a stationary target without vestibular stimulation was subtracted from the predicted discharge in **a**, **c**. In **b**, **d** fit sine function is shown for each discharge. For further explanation, see text

VOR cancellation and VOR ×1 was basically similar (Fig. 6a–d).

It has been shown that discharge of floccular gaze velocity Purkinje cells is approximated by linear addition of

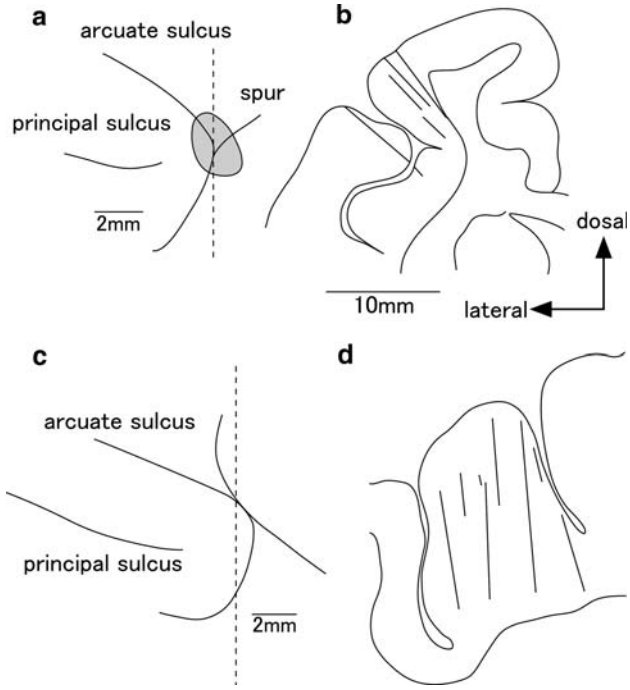

Fig. 7 Recording locations of 2 monkeys. **a**, **b** and **c**, **d** are from different monkeys. **a** and **c**, top view of the left peri-arcuate cortex. The *grey* area in **a** indicates entry points of tracks. **b** and **d**, cross sections through areas indicated by *dashed lines* in **a** and **c**, respectively, showing trajectory of tracks containing responsive neurons

discharge modulation during fronto-parallel pursuit and VOR ×1 (Lisberger and Fuchs 1978). FEF pursuit neurons exhibited similar addition during rotational VOR cancellation (Akao et al. 2007). Similar addition was also observed during right/left translational VOR cancellation in the seven neurons as shown in Fig. 6a, blue (also Fig. 6c for the six neurons: blue for rotational VOR cancellation).

Recording location

Figure 7 illustrates the recording tracks of the 2 monkeys (a, b, c, d). Responding neurons were found in the fundus of the arcuate sulcus and the area dorsal to the superior arcuate sulcus and spur (Fig. 7b, d). These areas are similar to those reported in previous studies for pursuit neurons responsive to whole body rotation (Fukushima et al. 2000; also Ebata et al 2004).

Discussion

The present study has demonstrated for the first time that the majority of FEF pursuit neurons in alert monkeys were activated by passive whole body translation without a target in complete darkness (Figs. 1, 3, Table 1B). These responses

were not a result of translational VOR for the following reasons. (1) Vergence eye velocity was induced minimally during fore/aft translation without a target (Fig. 1e, i). (2) There was no correlation between sensitivity of these neurons to chair velocity during fore/aft and right/left translation and simultaneously evoked translational VOR (Fig. 2c–g). (3) During translation at different orientations (Fig. 3), discharge modulation was not accounted for by simultaneously recorded translational VOR. (4) During right/left translation and fore/aft translation with a target, nearly all neurons tested (13/14) discharged when the monkeys cancelled VOR by fixating a target that moved together with whole body during which eye velocity was induced minimally (Figs. 5, 6), and (5) during translational VOR ×1 also, discharge of FEF pursuit neurons cannot be accounted for by eye velocity sensitivity alone (e.g., Fig. 5a vs. c, k vs. m). It is well known that horizontal whole body translation selectively activates the otolith organ, especially, utriculus (see Wilson and Melvill Jones 1979 for a review). Therefore, our results indicate that otolith inputs contributed to the discharge modulation of FEF pursuit neurons to horizontal translation in complete darkness.

Previous studies in our laboratory have shown that the majority of pursuit neurons in the caudal FEF respond to semi-circular canal inputs induced by passive whole body rotation in complete darkness and that preferred directions to semi-circular canal inputs and pursuit-preferred directions are similar (Fukushima et al. 2000; Akao et al. 2007). The present results show that there was no obvious directional correlation between discharge modulation induced by fore/aft and right/left translation and vergence-pursuit/horizontal-pursuit preferred directions (Fig. 2c–e). Our results has demonstrated that preferred directions of translational responses of FEF pursuit neurons were distributed nearly evenly in front of the monkeys (Fig. 4). We rarely obtained neurons with preferred directions oriented backward of the monkeys (Fig. 4). It is possible that pursuit related neurons do not need to know about targets and movements behind the animal where it cannot see. However, because during fore/aft translation some FEF pursuit neurons discharged during backward translation (Fig. 2a, phase near ±180°), it is also possible that the lack of neurons with preferred directions oriented backward of the monkeys was due to our small sample. In the present study, we are unable to determine whether some FEF pursuit neurons had a vertical preferred direction due to the limitations of our experimental apparatus. Nevertheless, our results suggest a difference in the way otolith and semi-circular canal inputs are represented in FEF pursuit neurons (see below).

It has been shown that the majority of FEF pursuit neurons signal gaze velocity during passive whole body rotation (Fukushima et al. 2000, 2008; Akao et al. 2007) with discharge characteristics similar to floccular gaze velocity Purkinje cells (Miles and Fuller 1975; Lisberger and Fuchs 1978). Comparison of discharge modulation during right/left translational VOR cancellation and VOR ×1 revealed that half of FEF pursuit neurons tested in the present study (7/14) exhibited discharge characteristics similar to gaze velocity neurons (Fig. 5a–c, f–h). Moreover, discharge of these neurons during translational VOR cancellation was approximated by linear addition of discharge modulation during fronto-parallel pursuit and translational VOR ×1 (Fig. 6a). These results suggest that some FEF pursuit neurons signal gaze velocity during right/left translation as well as whole body rotation.

The pathway of otolith input to FEF remains to be determined. Similar preferred directions have been reported for many neurons in the medial superior temporal (MST) cortical area that respond to passive whole body translation (Duffy 1998; Page and Duffy 2003; Gu et al. 2006). Reciprocal connections between the FEF and MST (Tusa and Ungerleider 1988; Stanton et al. 1993, 1995; Tian and Lynch 1996a, b) may transmit otolith signals from MST to FEF pursuit neurons.

Otolith and semi-circular canal signals to the FEF pursuit area may, at least in part, be transmitted by direct projections from the thalamus. Such projections have been suggested by anatomical and electrophysiological studies in rats and monkeys (Shiroyama et al. 1999; Ebata et al. 2004; also, de Waele et al. 2001 in humans). Latencies of vestibular responses of FEF pursuit neurons induced by whole body ramp rotation (~20 ms, Akao et al. 2007) are consistent with such direct projections (also, Fukushima et al. 2008 for head only rotation). Further studies are needed to examine latencies of otolith responses of FEF pursuit neurons induced by whole body ramp translation. Also, to understand the role of otolith inputs to the caudal FEF, future studies are needed to test the effects of target distance on discharge modulation of FEF pursuit neurons during whole body translation. The difference in the way otolith and semi-circular canal inputs are conveyed to FEF pursuit neurons as discussed above may be related to the difference in requirement of translational and rotational VOR (see Angelaki 2004 for a review).

Acknowledgments This research was supported by Grant-in-Aid for Scientific Research on Priority Areas (System study on higher-order brain functions) (17022001) from the MEXT of Japan.

References

Akao T, Kurkin S, Fukushima J, Fukushima K (2005) Visual and vergence eye movement related responses of pursuit neurons in the caudal frontal eye fields to motion-in-depth stimuli. Exp Brain Res 164:92–108

Akao T, Saito H, Fukushima J, Kurkin S, Fukushima K (2007) Latency of vestibular responses of pursuit neurons in the caudal frontal eye fields to whole body rotation. Exp Brain Res 177:400–410

Angelaki DE (2004) Eyes on target: What neurons must do for the vestibuloocular reflex during linear motion. J Neurophysiol 92:20–35

Angelaki DE, Green AM, Dickman JD (2001) Differential sensorimotor processing of vestibulo-ocular signals during rotation and translation. J Neurosci 21:3968–3985

Colby CL, Duhamel L, Goldberg ME (1993) Ventral intraparietal area of macaque: anatomic location and visual response properties. J Neurophysiol 69:902–914

de Waele C, Baudonniere PM, Lepecq JC, Huy PTB, Vidal PP (2001) Vestibular projections in the human cortex. Exp Brain Res 141:541–551

Duffy CJ (1998) MST neurons respond to optic flow and translational movement. J Neurophysiol 80:1816–1827

Ebata S, Sugiuchi Y, Izawa Y, Shinomiya K, Shinoda Y (2004) Vestibular projection to the periarcuate cortex in the monkey. Neurosci Res 49:55–68

Fuchs AF, Robinson DA (1966) A method for measuring horizontal and vertical eye movements chronically in the monkey. J Appl Physiol 21:1068–1070

Fukushima J, Akao T, Kurkin S, Kaneko CRS, Fukushima K (2006) The vestibular-related frontal cortex and its role in smooth-pursuit eye movements and vestibular-pursuit interactions. J Vestibular Res 16:1–22

Fukushima K, Sato T, Fukushima J, Shinmei Y, Kaneko CRS (2000) Activity of smooth pursuit-related neurons in the monkey periarcuate cortex during pursuit and passive whole body rotation. J Neurophysiol 83:563–587

Fukushima K, Yamanobe T, Shinmei Y, Fukushima J, Kurkin S, Peterson BW (2002a) Coding of smooth eye movements in three-dimensional space by frontal cortex. Nature 419:157–162

Fukushima K, Yamanobe T, Shinmei Y, Fukushima J (2002b) Predictive responses of periarcuate pursuit neurons to visual target motion. Exp Brain Res 145:104–120

Fukushima K, Akao T, Kurkin S, Fukushima J (2005) Role of vestibular signals in the caudal part of the frontal eye fields in pursuit eye movements in three-dimensional space. Ann NY Acad Sci 1039:272–282

Fukushima K, Kasahara S, Akao T, Kurkin S, Fukushima J, Peterson BW (2008) Eye-pursuit and re-afferent head movement signals carried by pursuit neurons in the caudal part of the frontal eye fields during head-free pursuit. Cerebral Cortex, doi: 10.1093/cercor/bhn079

Gottlieb JP, Bruce CJ, MacAvoy MG (1993) Smooth eye movements elicited by microstimulation in the primate frontal eye field. J Neurophysiol 69:786–799

Gottlieb JP, MacAvoy MG, Bruce CJ (1994) Neural responses related to smooth pursuit eye movements and their correspondence with electrically elicited slow eye movements in the primate frontal eye field. J Neurophysiol 72:1634–1653

Gu Y, Watkins PV, Angelaki DE, DeAngelis GC (2006) Visual and nonvisual contributions to three-dimensional heading selectivity in the Medial Superior Temporal area. J Neurosci 26:73–85

Leigh RJ, Zee DS (2006) The neurology of eye movements, 3rd edn. Oxford Univ Press, New York

Lisberger SG, Fuchs AF (1978) Role of primate flocculus during rapid behavioral modification of vestibuloocular reflex. I. Purkinje cell activity during visually guided horizontal smooth-pursuit eye movements and passive head rotation. J Neurophysiol 41:733–763

MacAvoy MG, Gottlieb JP, Bruce CJ (1991) Smooth pursuit eye movement representation in the primate frontal eye field. Cerebral Cortex 1:95–102

Miles FA, Fuller JH (1975) Visual tracking and the primate flocculus. Science 189:1000–1003

Miyamoto T, Fukushima K, Takada T, de Waele C, Vidal P-P (2007) Saccular stimulation of the human cortex: a functional magnetic resonance imaging study. Neurosci Lett 423:68–72

Page WK, Duffy CJ (2003) Head representation in MST: sensory interactions and population encoding. J Neurophysiol 89:1994–2013

Shiroyama T, Kayahara T, Yasui Y, Nomura J, Nakano K (1999) Projections of the vestibular nuclei to the thalamus in the rat: a phaseolus vulgaris leucoaggulutinin study. J Comp Neurol 407:318–332

Stanton GB, Bruce CJ, Goldberg ME (1993) Topography of projections to the frontal lobe from the macaque frontal eye fields. J Comp Neurol 330:286–301

Stanton GB, Bruce CJ, Goldberg ME (1995) Topography of projections to posterior cortical areas from macaque frontal eye fields. J Comp Neurol 353:291–305

Tanaka M, Fukushima K (1998) Neuronal responses related to smooth pursuit eye movements in the periarcuate cortical area of monkeys. J Neurophysiol 80:28–47

Tanaka M, Lisberger SG (2002) Role of arcuate frontal cortex of monkeys in smooth pursuit eye movements. I. Basic response properties to retinal image motion and position. J Neurophysiol 87:2684–2699

Tian J, Lynch JC (1996a) Functionally defined smooth and saccadic eye movement subregions in the frontal eye field of Cebus monkeys. J Neurophysiol 76:2740–2771

Tian J, Lynch JC (1996b) Corticocortical input to smooth and saccadic eye movement subregions of the frontal eye field in Cebus monkeys. J Neurophysiol 76:2754–2771

Tomko DL, Paige GD (1992) Linear vestibuloocular reflex during motion along axies between nasooccipital and interaural. Ann NY Acad Sci 656:233–241

Tusa RJ, Ungerleider LG (1988) Fiber pathways of cortical areas mediating smooth pursuit eye movement in monkeys. Ann Neurol 23:174–183

Wilson VJ, Melvill Jones G (1979) Mammalian vestibular physiology. Plenum press, New York

Wilson VJ, Ezure K, Timerick SJB (1984) Tonic neck reflex of the decerebrate cat: response of spinal interneurons to natural stimulation of neck and vestibular receptors. J Neurophysiol 51:567–577